



Short communication

A 4-cell miniature direct formic acid fuel cell stack with independent fuel reservoir: Design and performance investigation

Ping Hong, Yiliang Zhong, Shijun Liao*, Jianhuang Zeng, Xueyi Lu, Wei Chen

School of Chemistry and Chemical Engineering, South China University of Technology, Guangzhou 510641, China; Key lab for fuel cell technology of Guangdong Province & Key lab of enhanced heat transfer and energy conservation, Ministry of Education, China

ARTICLE INFO

Article history:

Received 3 March 2011

Accepted 7 March 2011

Available online 15 March 2011

Keywords:

Air-breathing

Direct formic acid fuel cell (DFAFC)

Stack

Dynamic response

ABSTRACT

A miniature air-breathing direct formic acid fuel cell (DFAFC) based 4-cell stack, with a gold coated printed circuit board as the end plate and current collector, and with an independent fuel reservoir to avoid undesired interlaced electrolysis between different cells, is designed and investigated. Emphasis in the investigation is placed on design details, cell performance, dynamic response, and the stability of both the stack and individual cells. The striking difference in our cell configuration as compared with constructions reported in the literature is the existence of independent cavities as fuel reservoirs for each single cell. The outstanding merit of this particular design is the avoidance of water hydrolysis between electrodes, which is inevitable in stacks built with a shared fuel tank. A maximum power density of 56.6 mW cm^{-2} is achieved and 5.0 M is considered as the optimum concentration for this 4-cell stack. A single cell can discharge at 20 mA for 70 h with a voltage decline rate of only 2.7 mV h^{-1} while sufficient formic acid is pumped into the cell.

© 2011 Elsevier B.V. All rights reserved.

1. Introduction

The swiftly growing market for portable electronic products (such as smart phones, tablet PCs, digital cameras, laptops, and so on) has stimulated the rapid development of long-lasting power devices. Such devices, with their high energy density and compactness, are the base on which the sophisticated functions of these electronic products are carried out. One of the power options is the direct liquid fuel cell (DLFC), since it has very high power density (relative to a lithium battery) and theoretically can run as long as liquid fuel is fed into the cell. In this regard, direct alcohol (methanol and ethanol) fuel cells have been extensively investigated and some of these have progressed to the frontier of commercial application. However, methanol is toxic and permeable through Nafion membrane (the main reason for decreased performance). Ethanol oxidation on the catalysts is a very slow process since it is a 6-electron reaction. In comparison, direct formic acid fuel cells (DFAFCs) display a wide spectrum of advantages because of formic acid's inherent characteristics, including fast electro-oxidation [1], low fuel crossover through Nafion membrane [2,3], nonflammability, and ease of fuel availability [4–6]. The passive air-breathing DFAFC in particular is more attractive and competitive [7–9] due to

the added advantage of operation without auxiliary devices (such as pumps for feeding fuel and air fans for system cooling, which are used in active fuel cells) [10]. These benefits make the passive DFAFC lighter and smaller relative to its active counterpart.

The inherent properties of printed circuit boards (PCBs), such as high strength, good machinability, and light weight, make them suitable candidates for use as end plates and current collectors. Previous studies [11–13] have demonstrated the successful application of PCB technology in direct methanol fuel cells (DMFCs) and proton exchange membrane fuel cells (PEMFCs). Our recent studies [14,15] also confirmed that using a gold layer coated PCB as an end plate and current collector was feasible in a passive DFAFC.

The output voltage or power for an electrical appliance has to reach a certain threshold value to operate and this is normally carried out by combining single cells together in series or in parallel. Of the different connection methods reported, the majority involve the use of either a bipolar or a monopolar plate. The bipolar structure was mainly adopted in active mode fuel cells. Miesse et al. [16] reported a DFAFC portable power system with 15 cells interconnected using bipolar plates, and found that the hybrid system produced 30 W at 60 mW cm^{-2} and powered a laptop computer for over 150 min. However, a bipolar plate cannot be used in a passive mode DLFC since one end of the polar plate has to breathe air [17]. A monopolar plate structure is a conventional stack design mode for a passive DLFC [17–20]. Chan et al. [20] reported a small DMFC stack using monopolar plates, with 6 cells sharing one fuel tank. To ensure the even distribution of methanol, individual cells were interconnected to achieve uniform fuel concentration. The authors

* Corresponding author at: South China University of Technology, School of Chemistry and Chemical Engineering, Wushan, Guangzhou 510641, China. Tel.: +86 20 8711 3586; fax: +86 20 8711 2906.

E-mail address: chsjliao@scut.edu.cn (S. Liao).

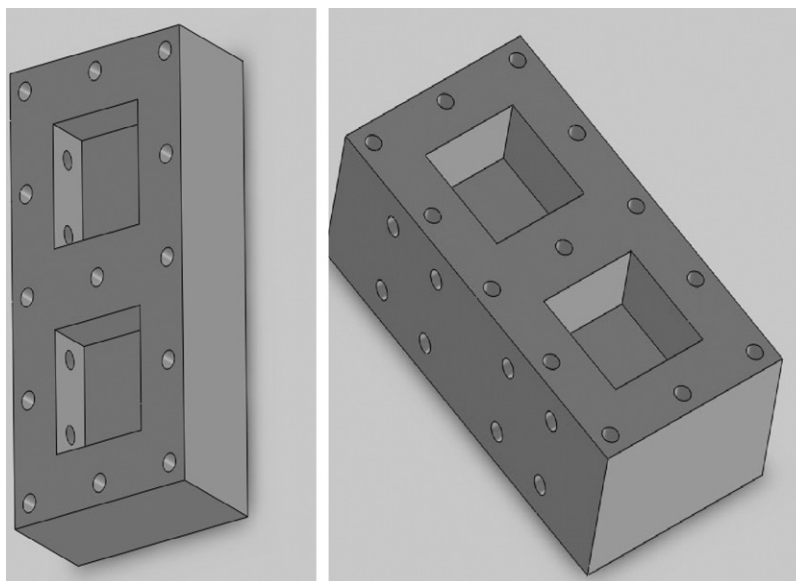


Fig. 1. Illustrations of the fuel reservoir, created by AutoCAD software.

in this work also designed a twin-cell stack that consisted of 2 “face-to-face” single cells with one shared fuel reservoir [15]. The output voltage could be maintained at 1.14 V for about 5 h (discharging at 20 mA by being fed 3.5 ml 5.0 M formic acid solution) and this performance could almost be reproduced when fresh fuel was injected. More single cells are needed in series to obtain a higher voltage. However, water electrolysis in the fuel is a possibility since the potential between the two electrodes is higher than 1.2 V [21]. Theoretically, water electrolysis will take place if more than 3 single cells are connected in series with one shared fuel reservoir [15,20]. Compared with a DMFC, the situation in a DFAFC would be much worse because formic acid is a good electrical conductor. Therefore, having an independent fuel reservoir for each single cell is better than a combined fuel tank design, and is probably the key for a multi-cell passive DFAFC stack to operate in practice.

It is understandable that the capability of a stack in series is determined by the cell that provides the worst performance, and stack degradation can be ascribed to that single cell [12]. Previous studies [12,17,20] have reported this observation and attributed it to the non-uniform distribution of the contact pressure between cells. We think this non-uniform distribution probably results from the uneven distribution of hold-down bolts, in other words, this uneven distribution may be the origin of the problem. A tailor-made stack structure is needed to provide symmetry for each cell, including the fuel and air supply, applied pressure, and so on. Against this background, we designed a fuel reservoir with four separated cavities for each single cell and then assembled a 4-cell stack based on PCB technology. This design is apparently advantageous over a stack simply constructed using 4 single cells in series, as in ref. [14], since it significantly reduces cell volume and weight. Symmetrical construction guarantees even distribution of pressure and ensures the uniformity of each single cell. We also studied the dynamic performance of the stack and long-term performance of a single cell while sufficient formic acid was fed by pumping.

2. Experimental

2.1. Fuel reservoir design and stack assembly

The functions of the fuel reservoir were to store the fuel and provide support for each single cell. Fig. 1 shows illustrations of the fuel reservoir, created by AutoCAD software. The illustrations

present different viewgraphs of the reservoir from left and right. In this work, four cavities were placed back-to-back in the two sides of the fuel reservoir, as shown in Fig. 1. They were all independent and not interconnected, thus preventing possible electrolysis of water in the fuel. The volume capacity of each cavity was 3.5 cm³ (length: 2.1 cm, width: 2.1 cm, and depth: 0.8 cm). In the top of each cavity, two circular holes ($\varnothing 2$ mm) were used as the fuel entrance and gas exit. A syringe was used to inject the reactant, formic acid, through the holes to the cavity, while CO₂ created during the reaction was released to the environment via the holes.

The 4 single cells, gaskets, and fuel reservoir were assembled using 13 stainless steel bolts inserted through small circular holes, as shown in Fig. 2. Gold coated PCBs were used as the current collectors and end plates. More details about the stack design and the function of the gold coated PCBs can be found in our previous reports [14,15]. Fig. 3 shows a zoomed-in view of the assembled 4-cell stack. For quick reference, a single cell is denoted as Cell X where X is from 1 to 4. The anode wire of Cell X (X=1, 2, or 3) was connected to the cathode wire of Cell X+1 (for example, the anode wire of Cell 1 was connected to the cathode wire of Cell 2 and so forth) and the remaining two wires were connected to the external circuit for performance testing. The stack was 7.5 cm long,

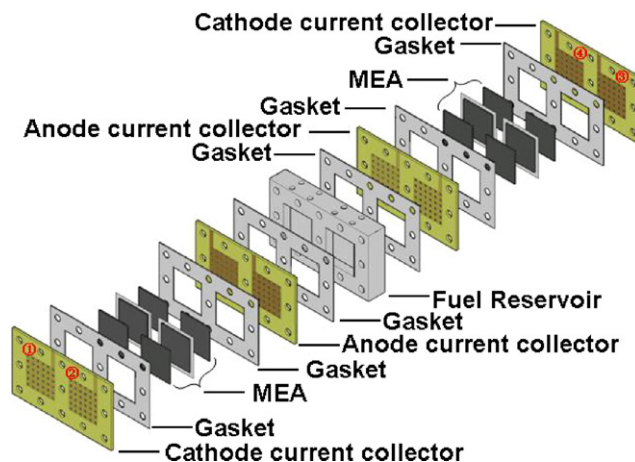


Fig. 2. Schematic of the 4-cell stack.

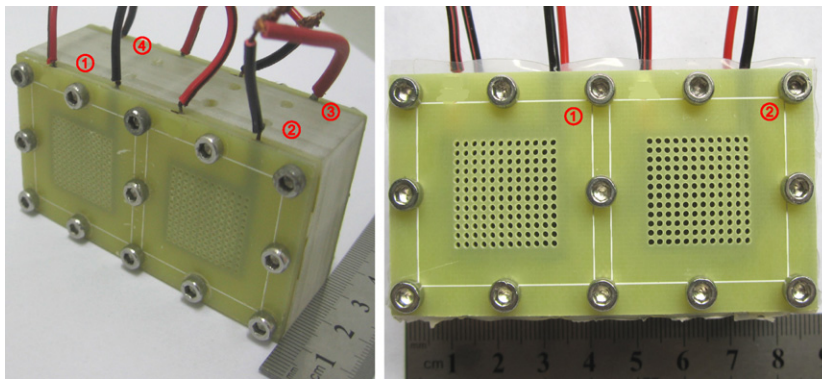


Fig. 3. Miniature air-breathing DFAFC 4-cell stack developed in this study.

3.0 cm wide, and 4.0 cm high. The 4 single cells could discharge individually as the wires were not connected together.

2.2. Membrane electrode assembly

The membrane electrode assembly (MEA) was prepared using a “direct catalyst spraying” technique developed in our group [22]. The catalyst used at the anode and cathode was 40 wt.% Pt/C sourced from Johnson Matthey and the catalyst loading was kept at 2.0 mg cm^{-2} in each electrode. The effective area of each MEA was 4 cm^2 . Pristine and hydrophobic carbon paper was used as a diffusion layer in the anode and cathode respectively. More details about the MEA and diffusion layer preparation can be found elsewhere [15].

2.3. Stack performance test

Formic acid (Enox[®], 88% analytical grade, China) was diluted with deionized water to form aqueous solutions ranging from 2.0 to 8.0 M. A given solution was then fed into each cavity at the same time. Before the performance measurement, the stack was left to condition for 10 min at room temperature. The open circuit voltage (OCV) of the stack and each single cell was recorded by a high-precision cell testing system (Neware[®], CT-3008W-5V1A-S4, China). The cell performance curve (I - V) was recorded on a homemade electrochemical workstation in galvanostatic discharging mode with a current range of 5 to 440 mA at uneven intervals. At each step, the cell was discharged for 20 s, followed by a rest for 60 s before the next step. Voltage data were collected at 0.5 s intervals and then averaged to plot the I - V curve.

2.4. Dynamic and long-term performance tests

Dynamic and long-term performance was determined through a high-precision cell testing system using galvanostatic testing. For the dynamic test, the current was set at 60 mA, 40 mA, or 20 mA, and the stack was allowed to discharge for 30 min at each current. The long-term discharging test was performed using a constant current of 20 mA. The voltages of the stack and single cells were recorded on-line during these processes. To investigate cell stability and eliminate the effect of gradual fuel consumption, 2 L 5.0 M HCOOH was fed circularly by pumping while the voltage was recorded as the single cell discharged at 20 mA.

3. Results and discussion

3.1. OCV behavior

The diffusion layers and MEAs were all dried before the performance tests, formic acid solution was injected into the fuel reservoir

within 3 s. The OCVs of the stack and single cells were recorded at the moment of fuel injection, as in Fig. 4. It can be seen that the OCV of the stack jumped from zero at the beginning to approximately 3.20 V in 60 s, then dropped to a stable value of 2.75 V in 140 s. The OCV curves of the single cells showed a similar behavior. OCV peak formation is a combined result of MEA humidification, formic acid crossover, and cell temperature. The previously dried MEAs became wet when the fuel was injected into the reservoir at the anode, and the OCV accordingly changed quickly to a peak value. With the injection of formic acid, permeation of formic acid from anode to cathode became inevitable and the permeated formic acid then reacted with oxygen in the cathode, leading to a decrease in OCV by producing a mixed potential. In the meantime, cell temperature increased due to the reaction. The increased temperature enhanced the electrochemical kinetics at both electrodes and increased the rate of fuel crossover [23]. The combined effect led to a relatively stable OCV. Fig. 4 also shows that the OCV of each single cell in the stack almost overlaps, an indication of cell uniformity (at 500 s, Cell 1: 0.63 V, Cell 2: 0.68 V, Cell 3: 0.67 V, Cell 4: 0.68 V). It has been reported that cell uniformity in a stack is a prerequisite for yielding similar performance in the single cell [20]. Hereafter, stable OCVs for the single cell were collected to detect cell uniformity after the stack was left to condition for about 10 min.

3.2. Effects of formic acid concentration on stack performance

Fig. 5 shows the performance of the 4-cell stack operated with different formic acid concentrations, from 2.0 M to 8.0 M. In the zoomed-in view it can be seen that the OCV decreased from 2.72 V

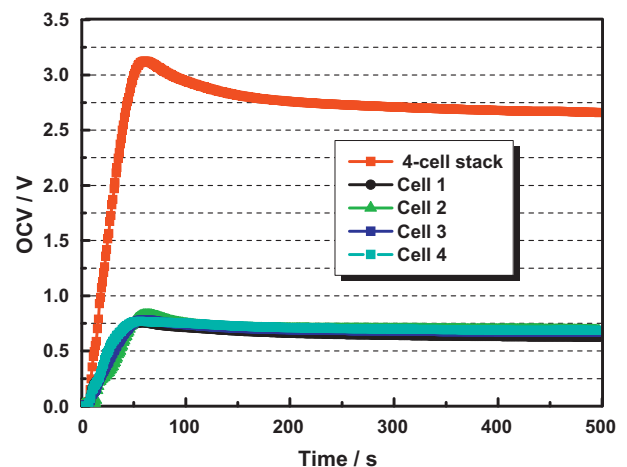


Fig. 4. OCV of the stack and single cells after fuel supply at room temperature (5.0 M HCOOH).

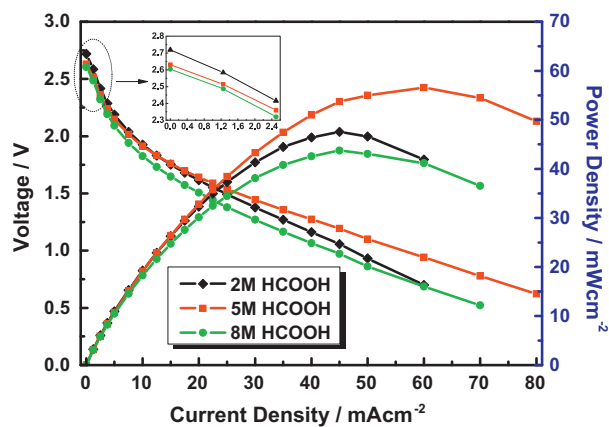


Fig. 5. The effect of formic acid concentration on the performance of the stack.

to 2.60V with increasing formic acid concentration. The maximum power density increased from 47.6 mW cm^{-2} at 2.0M to 56.6 mW cm^{-2} at 5.0M, then decreased to 43.8 mW cm^{-2} at 8.0M. Possible explanations for these differences are the combined effects of fuel crossover, stack temperature, and fuel supply rate. It is known that the rate of formic acid crossover from anode to cathode increases with formic acid concentration [2,3]. The mixed potential on the cathode side is prorated in proportion to the permeated formic acid, consequently lowering the stack's OCV. However, this adverse effect should be negligible at low concentrations. Meanwhile, the heat generated by the exothermic reaction between the permeated formic acid and oxygen results in increased stack working temperature, which is beneficial for increasing the rate of formic acid oxidation and oxygen reduction. The abovementioned pros and cons are conducive to better performance at 5.0M than at 2.0M, especially at high current densities. Decreased performance occurred at 8.0M because the effect of mixed potential predominated over the effect of temperature increase. This indicated that 5.0M might be the optimum concentration for this 4-cell stack. Thereafter in this study we used 5.0 M formic acid as the electrolyte.

3.3. Dynamic response test

Fig. 6 shows the dynamic response of the stack voltage under a discharging current decreasing from 60 mA to 20 mA as 3.5 ml 5.0M HCOOH was fed into each single cell. The stack was able to work at different constant currents with relatively stable voltages. The stack discharged at 60 mA after the initial 30 min, and the voltage went from 1.56 V to a relatively stable plateau (1.62 V), then dropped to 1.59 V. However, the voltage at a lower discharging current decreased as time proceeded (40 mA: from 1.79 V to 1.70 V; 20 mA: from 1.98 V to 1.91 V). The voltage could be maintained at a relatively stable level perhaps because the temperature rose rapidly, which contributed to fast formic acid oxidation and oxygen reduction. It is noteworthy that the supply of formic acid at the beginning should be abundant and pose no limitation to the reaction rate increase. Possible reasons for the voltage decline at low discharging current could be limited heat generation from the formic acid oxidation reaction and a high over-potential that oxidizes adsorbed poisoning species on the anode catalyst [24,25].

3.4. Stack long-term performance

Fig. 7 shows the long-term performance of the stack discharging at a constant current of 20 mA as 3.5 ml 5.0 M HCOOH was fed to each single cell. The voltages of individual cells were recorded at the same time. It can be seen that the voltage decrease can be

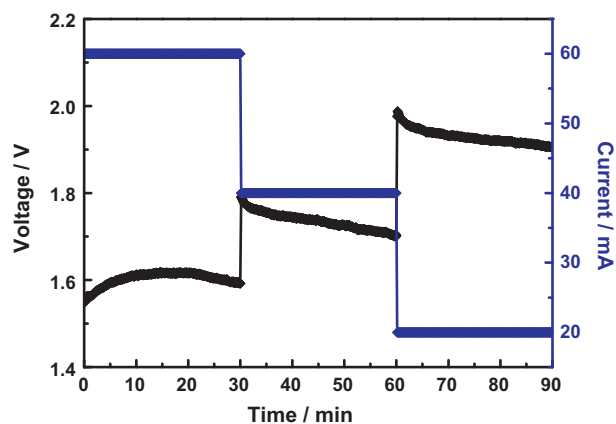


Fig. 6. Dynamic response of 4-cell stack under decreasing current steps (from 60 mA to 20 mA).

divided into three distinct stages. The voltage dropped quickly from 2.56 V to 2.10 V in the first few minutes, then decreased gradually from 2.10 V to 1.75 V during the following 7 h at a rate of ca. 0.05 V h^{-1} . Finally, the voltage dropped quickly again from 1.75 V to 1.20 V in 3 h at an average rate of ca. 0.18 V h^{-1} . Cell performance degradation is a combination of many contributing factors, including decreased formic acid concentration, catalyst dissolution and poisoning, fuel crossover, and water accumulation at the cathode [7,26]. These factors are interrelated and optimized cell performance can be obtained when a fine balance of these factors is maintained. Fig. 7 also shows the voltage contribution of each single cell during the stack discharging process. The similar performance further confirmed the uniform performance of the single cells, probably due to the symmetrical stack design.

3.5. Single cell discharging stability as cyclic fuel was fed

A practical fuel cell stack should be capable of providing stable and sustainable performance for a long time. As mentioned in Section 3.4, many reasons for stack performance degradation have been proposed. Limited fuel supply in the reservoir may be the prevailing reason. To confirm our hypothesis and to study the cell stability as sufficient formic acid was fed, we used a circulation pump to provide fresh fuel for Cell 1. The experiment was carried out by pumping 2 L 5.0M HCOOH (stored in a volumetric flask) into the cell with a circulating rate of 3 ml min^{-1} while the

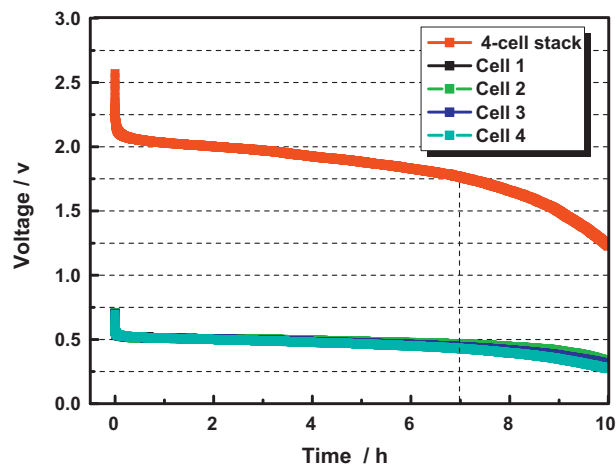


Fig. 7. Voltages of stack and each single cell as the stack discharged at a constant current of 20 mA.

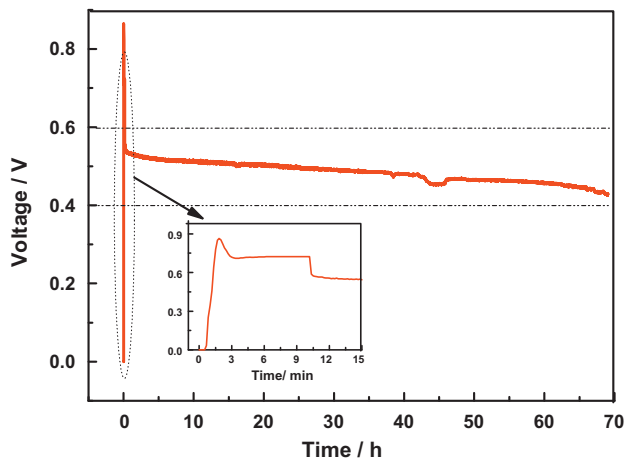


Fig. 8. The constant current discharging performance of a single cell when 2 L 5.0 M HCOOH was supplied circularly by pumping.

cell discharged at a constant current of 20 mA after 10 min of conditioning. At the same time, the voltage was recorded, as is shown in Fig. 8. The insert figure in the bottom left of Fig. 8 clearly shows the OCV behavior, which was similar in shape to the OCV in Fig. 4. After conditioning for 10 min, the cell discharged at 20 mA, exhibiting an initial voltage of 0.60 V. Voltage decline occurred from 0.60 V to 0.41 V at a degradation rate of 2.7 mV h^{-1} during the following 70 h, whereas the formic acid concentration decreased slightly from 5.0 M to 4.8 M, as measured by titration. It therefore can be concluded that under the condition of a minor and negligible decrease in formic acid concentration, decay in cell performance was most probably due to degradation of the catalysts and/or MEA structural change during the long-term discharging process. On the other hand, the experiment provided indirect proof of the reason for the performance degradation described in Section 3.4, i.e. fuel consumption. A passive stack may discharge for a long time, provided that it is fed sufficient fuel. Future work focusing on in-depth analysis of cell degradation is still in progress, but the experimental results demonstrated in this study have provided new insight into the design of viable DFAFCs.

4. Conclusions

A miniature air-breathing DFAFC stack consisting of 4 single cells in series was designed and tested. The effect of formic acid concentration on cell performance was studied and it was found that 5.0 M might be the optimum concentration for this 4-cell stack. The stack voltage decreased only about 20% (from 2.56 V to 1.20 V) in 10 h at a constant discharging current (20 mA), an indication of good stability. Each single cell displayed a similar voltage profile, probably resulting from the symmetrical stack design. The main reason for

stack performance degradation was found to be fuel consumption. It is therefore concluded that the stack design reported in this work is viable for practical situations and can potentially be applied in the portable electronic device market.

Acknowledgements

We would like to thank the National Natural Science Foundation of China (Project Nos. 20673040, 20876062, and 21076089), the Ministry of Science and Technology of China (Project No. 2009AA05Z119), and the Department of Science and Technology of Guangdong Province (Project No. 2004A11004003) for their financial support of this work. We also thank Dr. Richu Gu, Xinjian Huang, and Xiaowei Wang for their assistance in preparing the reservoirs and the gold coated PCBs.

References

- [1] U.B. Demirci, *J. Power Sources* 169 (2007) 239–246.
- [2] K.J. Jeong, C.M. Miesse, J.H. Choi, J. Lee, J. Han, S.P. Yoon, S.W. Nam, T.H. Lim, T.G. Lee, *J. Power Sources* 168 (2007) 119–125.
- [3] Y.W. Rhee, S.Y. Ha, R.I. Masel, *J. Power Sources* 117 (2003) 35–38.
- [4] J.S. Kim, J.K. Yu, H.S. Lee, J.Y. Kim, Y.C. Kim, J.H. Han, I.H. Oh, Y.W. Rhee, *Korean J. Chem. Eng.* 22 (2005) 661–665.
- [5] S. Ha, B. Adams, R.I. Masel, *J. Power Sources* 128 (2004) 119–124.
- [6] C. Rice, S. Ha, R.I. Masel, P. Waszczuk, A. Wieckowski, T. Barnard, *J. Power Sources* 111 (2002) 83–89.
- [7] Y.Y. Kang, M.J. Ren, T. Yuan, Y.J. Qiao, Z.Q. Zou, H. Yang, *J. Power Sources* 195 (2010) 2649–2652.
- [8] J. Yeom, R.S. Jayashree, C. Rastogi, M.A. Shannon, P.J.A. Kenis, *J. Power Sources* 160 (2006) 1058–1064.
- [9] S. Ha, Z. Dunbar, R.I. Masel, *J. Power Sources* 158 (2006) 129–136.
- [10] L. Jaeyoung, H. Jonghee, C.M. Miesse, J. Won Suk, J. Kyoung-Jin, L. Jae Kwang, Y. Sung Pil, N. Suk Woo, L. Tae-Hoon, H. Seong-Ahn, *J. Power Sources* 162 (2006) 532–540.
- [11] A. Schmitz, S. Wagner, R. Hahn, H. Uzun, C. Hebling, *J. Power Sources* 127 (2004) 197–205.
- [12] J.W. Guo, X.F. Xie, J.H. Wang, Y.M. Shang, *Electrochim. Acta* 53 (2008) 3056–3064.
- [13] F.L. Zhao, G.Q. Sun, L.K. Chen, B. Qin, G.X. Wang, S.L. Wang, S.H. Yang, Q. Xin, *Chin. J. Power Sources* 31 (2007) 201–204.
- [14] P. Hong, S.J. Liao, J.H. Zeng, X.J. Huang, *J. Power Sources* 195 (2010) 7332–7337.
- [15] P. Hong, S.J. Liao, J.H. Zeng, Y.L. Zhong, Z.X. Liang, *J. Power Sources* 196 (2011) 1107–1111.
- [16] C.M. Miesse, W.S. Jung, K.-J. Jeong, J.K. Lee, J. Lee, J. Han, S.P. Yoon, S.W. Nam, T.-H. Lim, S.-A. Hong, *J. Power Sources* 162 (2006) 532–540.
- [17] J.J. Martin, W. Qian, H. Wang, V. Neburchilov, J. Zhang, D.P. Wilkinson, Z. Chang, *J. Power Sources* 164 (2007) 287–292.
- [18] V. Baglio, A. Stassi, F.V. Matera, A. Di Blasi, V. Antonucci, A.S. Aricò, *J. Power Sources* 180 (2008) 797–802.
- [19] T. Tsujiguchi, M.A. Abdulkareem, T. Kudo, N. Nakagawa, T. Shimizu, M. Matsuda, *J. Power Sources* 195 (2010) 5975–5979.
- [20] Y.H. Chan, T.S. Zhao, R. Chen, C. Xu, *J. Power Sources* 178 (2008) 118–124.
- [21] H. Kim, M. Unlu, J.F. Zhou, I. Anestis-Richard, P.A. Kohl, *J. Power Sources* 195 (2010) 7289–7294.
- [22] L.M. Xu, S.J. Liao, L.J. Yang, Z.X. Liang, *Fuel Cells* 9 (2009) 101–105.
- [23] R. Chen, T.S. Zhao, *J. Power Sources* 167 (2007) 455–460.
- [24] J.H. Yoo, H.G. Choi, J.D. Nam, Y. Lee, C.H. Chung, E.S. Lee, J.K. Lee, S.M. Cho, *J. Power Sources* 158 (2006) 13–17.
- [25] J. Kalló, J. Kamara, W. Lehnert, R. von Helmolt, *J. Power Sources* 127 (2004) 181–186.
- [26] X.W. Yu, P.G. Pickup, *J. Power Sources* 182 (2008) 124–132.